RSC Advances

ROYAL SOCIETY OF CHEMISTRY

www.rsc.org/advances

Graphical and textual abstract

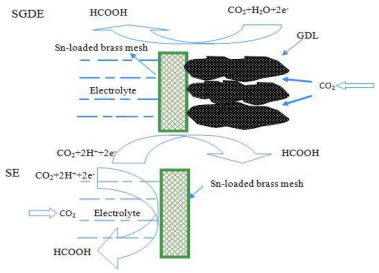

Using a two-layer gas diffusion electrode for ERCF in MEC, and the Faraday efficiency was improved by 36.1 %.

Enhanced Electrochemical Reduction of Carbon Dioxide to Formic Acid Using a Two-layer Gas Diffusion Electrode in Microbial Electrolysis Cell

Qinian Wang, Heng Dong*, Hongbing Yu*, Han Yu, Minghui Liu

College of Environmental Science and Engineering, Nankai University, No. 94 Weijin Road, Nankai District, Tianjin 300071, China

*Corresponding Authors; Phone: (86)22-23502756; Fax: (86)22-23502756; E-mail: dongheng@nankai.edu.cn; hongbingyu1130@sina.com.

ABSTRAC

Electrochemical reduction of CO_2 to formic acid (ERCF) is mainly hindered by CO_2 mass transfer and high energy consumption. This work developed a two-layer rolled Sn-loaded gas diffusion electrode (SGDE), consisting of a gas diffusion layer and a Sn-loaded brass mesh to improve ERCF in microbial electrolysis cell (MEC). The morphology and chemical composition of the SGDE were characterized by scanning electron microscope, X-ray diffraction, energy dispersive X-ray spectrometer and X-ray photoelectron spectroscopy. The electrochemical behavior of the SGDE for ERCF was assessed by cyclic voltammetry and electrochemical impedance spectroscopy. The Faraday efficiency and production yield of formic acid were measured in order to evaluate ERCF. The electrochemical measurements exhibited the advantages of the SGDE, including higher ERCF current and lower charge transfer resistance, owing to the increase in the working concentration of CO_2 in the vicinity of the electrocatalytically active sites. The use of the SGDE in MEC improved Faraday efficiency and production yield of formic acid by 36.1 % and 30.6 %,

respectively. Whereas the energy consumption for ERCF was reduced by approximately 67.2-73.6 %.

Keywords: electrochemical reduction; carbon dioxide; gas diffusion electrode; microbial electrolysis cell

1. Introduction

Electrochemical reduction of CO_2 to formic acid (ERCF) has gained great attention since it is a technically feasible and economically viable technique for valuable materials production and CO_2 offset [1-7]. To trigger ERCF in a common electrolytic cell (CEC) at the cathode where the anodic reaction is water oxidation, a minimum input voltage of ca. 2.5 V is needed [8]. Microbial electrolysis cell (MEC) has recently been proposed as a novel and sustainable technology for the renewable and sustainable production of biofuels or valuable chemicals from waste organic materials [9-11]. It consists of an anode and a cathode, which are typically separated by a proton exchange membrane (PEM). Different from the undesired water oxidation in CEC, an oxidized elimination of substrate by the bacteria accompanied with the release of electrons and protons occur on the bioanode in MEC. The electrons are then transferred to the cathode through an external circuit, while the protons diffuse to the cathode through the PEM. Finally, those electrons and protons are utilized in the reduction reactions of an electron acceptor at the cathode [12,13]. In most cases of MECs, with the assistance of the potential generates from substrate oxidation at the bioanode, lesser power supply is needed for the cathodic reactions than that in CEC. Take the hydrogen evolution reaction (HER) at the cathode in MEC as an example, the bacteria

at the anode consume organic matter and produce a potential of ca. - 0.3 V vs NHE, while HER requires a potential of -0.41 V vs NHE at pH 7.0, requiring a theoretical input voltage of 0.11 V. This voltage is substantially lower than that needed for HER from the electrolysis of water (1.21 V at pH 7.0 [14]). ERCF has been preliminary realized in MEC with an input voltage of ca 1.2-1.5 V [15,16], where Pb plates were used as the cathodes and CO_2 was provided by sparging in the catholyte bulk. As the solubility of CO_2 in water at ambient conditions is relatively low (ca. 0.033 M), CO_2 mass transfer from the bulk to the cathode surface is definitely a significant barrier for achieving an efficient ERCF in MEC. Several studies of ERCF in CEC have proposed gas diffusion electrodes (GDEs) as an effective method to alleviate CO_2 mass transfer limitation [17-20]. The fabricated GDEs were all of typical three-layer structure consisting of a gas diffusion layer (GDL), a current collector and a catalyst layer (CL). The CL was made of catalyst and binder, where ERCF occurred. Hydrophilic Nafion and hydrophobic polytetrafluoroethylene (PTFE) were the primary binders widely adopted in those GDEs [17-20]. The electron conduction and CO_2 diffusion in the CL are both very essential to ERCF [21]. However, Nafion and PTFE are non-conductor. Moreover, CO_2 diffusion in a Nafion-binded CL is insufficient since hydrophilic Nafion is unable to provide gas channel for CO_2 therein by itself [21]. Although using those typical GDEs have improved ERCF to a certain extent, the aforementioned problems concerning the CL have not be solved properly yet. In addition, it has been reported that the cost of cathode material accounts for about 47 % of overall investment in a bioelectrochemical system (e.g. MEC) [22]. Hence there is urgent need

to develop a GDE with low-cost and high performance for ERCF in MEC.

In this work, a two-layer Sn-loaded GDE (SGDE) without the traditional CL (e.g. without binder) was developed. The SGDE consists merely of a GDL and a brass mesh plated with Sn. We used Sn as the catalyst due to its high selectivity to ERCF and low risk to the environment and human health [19, 23]. Cyclic voltammetry (CV) and electrochemical impedance spectroscopy (EIS) were applied to assess its electrochemical behavior for ERCF. Constant potential electrolysis was adopted to evaluate ERCF in MEC. The Sn-loaded brass mesh (SE) without GDL was studied as control.

2. Experimental

2.1 Electrode preparation

The SGDE consisted of a GDL and a Sn-loaded brass mesh. The GDL was prepared as follows: conductive carbon black (Jinqiushi Chemical Co. Ltd., Tianjin, China) was distributed in a beaker with an appropriate amount of ethanol and ultrasonically agitated for 20 min. Then a PTFE suspension (60 wt%, Hesen, Shanghai, China) was dripped slowly into the beaker to form a blend. The mass ratio of conductive carbon black and PTFE was 3:7. This step was completed for 20 min. Then, the blend was stirred at 353 K to give a dough-like paste. The paste was then rolled to form a gas diffusion film of 0.15 mm thickness. The Sn-loaded brass mesh was made as follows: the brass mesh (60 mesh) was first immersed in acetone for 24 h and then etched in hydrochloric acid (10 %). Then, it was immersed in an electroless acidic tin plating bath, containting 0.02 M stannous sulphate, 0.22 M sulfuric acid and 0.6 M thiourea,

for 4 min at 319 K. The weights of the brass mesh before and after the loading process were also measured to control the loading of Sn catalyst and make the result more consistent. Finally, the Sn-loaded brass mesh was rolled on the GDL and sintered for 20 min at 613 K to obtain the final electrode of ca. 0.2 mm thickness.

2.2 MEC reactor construction and setup

The MEC reactor was derived from a two-chambered MFC reactor, which was constructed as previously described [24, 25]. The two compartments were separated by a PEM (Nafion117, Dupont, USA). The MFC was inoculated using a pre-acclimated bacterial suspension from MFCs which were operated for over one year. The reactor was fed with 50 mM phosphate buffer solution (PBS, Na_2HPO_4 4.09 g L^{-1}, $NaH_2PO_4 \cdot H_2O$ 2.93 g L^{-1}), trace minerals 12.5 mL L^{-1}, vitamins 5 mL L^{-1} and 1 g L^{-1} sodium acetate as substrate [26]. The external resistance was fixed at 1000 Ω by using a resistor box, except as indicated.

When the voltage of the two-chambered MFC became stable, the MFC operation was changed into MEC operation by replacing the cathode with the tested electrode (SGDE or SE, 7 cm^2) and the catholyte with 0.5 M $KHCO_3$ solution. The schematic overview of the MEC systems employed in this work is shown in the Supporting Information (Figure S1). For the SGDE, a gas chamber was specially designed (Figure S1b). The cathode and the bioanode were connected to the working electrode and the counter electrode of an electrochemical workstation (CHI600D, Shanghai Chenhua Instruments Co., China), respectively. The reference electrode was a Ag/AgCl electrode (sat. KCl, Tianjin Aidahengsheng Technology Co. Ltd., China)

and was electrolytically connected to the working electrode solution through a Luggin capillary.

2.3 ERCF in MEC

ERCF test in MEC was done under constant potential at 303 ± 1 K, using an electrochemical workstation (CHI600D, Shanghai Chenhua Instruments Co., China). The electrolyte was circulated using a peristaltic pump (BT-yz1515, Tianjin Sabo Instruments Co., China) at a flow rate of 25 mL min^{-1}. The flow rate of CO_2 (99.99 %, Tianjin Sizhi gas Co. Ltd., China) was 30 mL min^{-1}. The duration of each electrolysis run was 2 h. The catholyte was sampled for analysis after each run.

2.4 Analysis and calculations

The morphology of the SGDE was observed by SEM (S-3500N, Hitachi Limited, Japan). The crystal structure of the SGDE was characterized by XRD (Rigaku D/MAX-2500, Japan). The surface chemical composition of the SGDE was examined by EDX (IX2F-550I, EDAX Co., USA) and XPS (Axis Ultra DLD, Kratos Analytical Ltd., UK). The XPS data were analyzed by CasaXPS software.

The electrochemical behavior of the SGDE and SE for ERCF were assessed by CV and EIS, using an electrochemical workstation (CHI600D, Shanghai Chenhua Instruments Co., China). The experiments were carried out at ~ 298 K in a CEC, which was constructed as shown in Figure S1 except that a Pt sheet (1 cm^2, Tianjin Aidahengsheng Technology Co. Ltd., China) was used as counter electrode. The electrolyte in the cathodic chamber and anodic chamber was 0.5 M $KHCO_3$ solution. Before each measurement, where either the SGDE or the SE was used as working

electrode and the electrolyte was degassed with N_2 (99.99 %, Tianjin Sizhi gas Co. Ltd., China) for 30 min to obtain a baseline. During each measurement where the SE was used as working electrode, N_2 or CO_2 was continuously sparged in the electrolyte. When the SGDE was working electrode, N_2 or CO_2 was continuously fed into the gas chamber during the measurement. CV was conducted between 0 V and -2 V vs. Ag/AgCl at a scan rate of 0.1 V s^{-1} [19, 27]. EIS was performed over a frequency range of 100 kHz to 0.1 Hz with the AC signal amplitude of 0.005 V superimposed on different dc potentials of −1.2 V and −1.3 V vs. Ag/AgCl. The EIS data were analyzed using the Zsimpwin software (ver. 3.10).

The electrolytic production of formic acid was determined using a high performance liquid chromatography (HPLC, Beijing Puxitongyong Instruments Co., China) equipped with a C18 reversed phase column (250 mm×4.6 mm×5 μm) by using UV detector at 210 nm. The Faraday efficiency of formic acid production was calculated as previously described [15].

3. Results

3.1 SGDE characterization

SEM images of the SGDE show that the Sn-loaded brass mesh partially submerged in the GDL (Figure 1a). The Sn catalyst particles size was about 0.1-0.5 μm (Figure 1b) and the Sn film thickness was about 2-5 μm (Figure 1c). The XRD pattern of the SGDE (Figure S2) clearly showed the phase of Sn (JCPDS Card No.65-5224) and SnO_2 (JCPDS Card No.50-1429). SnO_2 was probably formed during the electrode annealing process. The Sn content in the Sn-loaded brass mesh of the SGDE was 6.45 %

(1.48 mg cm^{-2}), as determined by EDX analysis (Figure S3). The XPS spectrum of Sn3d exhibited peaks at binding energies 495.3 eV and 486.8 eV which can be assigned to Sn3d3/2 and Sn3d5/2, respectively (Figure S4). These energies are consistent with Sn (IV) bound to oxygen in SnO_2 [28]. Therefore Sn catalyst on the SGDE existed in the forms of SnO_2 and Sn, the former being in the external of the Sn-loaded brass mesh and the latter in the internal [29]. The SnO_2 layer is very essential for ERCF by assisting to thermodynamically stabilize CO_2^- intermediates as well as inhibit HER [29].

3.2 Electrochemical measurements

CVs obtained with the SGDE and the SE in N_2 environment are shown in Figure 2a. The reduction peaks appeared at -0.94 V and -1.28 V in turn while the oxidation peaks appeared at -0.92 V and -1.06 V. This should be caused by the irreversible redox reactions between Sn and tin oxides [30, 31]. It can be seen that the redox peak obtained from the SGDE was more obvious and broader than that from the SE, and the redox current from the SGDE was higher than that from the SE. This is possibly due to a higher electrochemically active species concentration for the redox reactions by using the SGDE than that by using the SE [19]. When scanning to the negative end of the voltammograms, a rapidly increase in the reduction currents can be observed for both electrodes, which should be caused by HER [32]. In the case of the SE, HER occurred at a potential more negative than ca. -1.4 V, which was by 0.3 V more positive than that in the case of the SGDE (ca. -1.7 V). This suggests that a higher overpotential was needed for HER with the SGDE than that with the SE. The HER current using the

SGDE was 35.7 %-41.5 % lower than that using the SE (Figure S5). The growing rate of HER obtained from the SGDE was also lower than that from the SE. These indicate that HER was hindered on the SGDE compared to the SE. When in CO_2 environment (Figure 2b), the rapidly increased currents were obtained from both electrodes at potentials more negative than ca. -1.2 V which should be contributed by both ERCF and HER [32]. The reduction current for the SGDE was higher than that for the SE at a potential more positive than -1.48 V. When the potential was negative than -1.48 V, the reduction current for the SGDE was lower than that for the SE. It can be seen that the growing rate of the reduction reactions for the SGDE increased when the potential shifted from -1.2 V to -1.3 V, but it decreased when the potential further shifted to more negative value (Figure S5). This should be attributed to the difference in HER for the SGDE and SE. Thus, it can be inferred that HER did not occur for both electrodes at a potential more positive than -1.3 V, and the reduction current in potential region from -1.2 V to -1.3 V should be caused by ERCF. The ERCF current for the SGDE was 19.5 % -62.7 % higher than that for the SE, which implies that the use of the SGDE can promote ERCF.

In order to further explore the electrochemical behavior of the SGDE and SE as it concerns ERCF, EIS measurements in CO_2 environment were carried out (Figure 3). All Nyquist plots consisted of two semicircles, indicating two time constants. The first one located at high frequencies (HF) and the second one at low frequencies (LF). It is clear to see that the HF semicircle was independent on the applied potential, whereas the diameter of LF semicircle considerably decreased as the applied potential was

199 decreased. Therefore, the HF semicircle probably represented the resistance of ionic
200 migration through the electrolyte film formed on the electrode/electrolyte interface
201 and the inner active sites. Whereas the LF semicircle, reflected the charge transfer
202 resistance of ERCF, which was dependent on the kinetics of reaction. All the Nyquist
203 plots have been modeled by the same equivalent circuit (Figure S6). According to this
204 equivalent circuit, the potential independent HF time constant was described by the
205 interfacial ohmic resistance (R_1) and constant phase element (CPE_1) connected in
206 parallel, whereas the potential dependent LF time constant was described by charge
207 transfer resistance (R_2) and CPE_2 connected in parallel. The parameters obtained from
208 the EIS fitting procedure are shown in Table S1. Just as expected, R_1 values at
209 different applied potentials for the SGDE and the SE were similar, respectively. On
210 the contrary, R_2 values were obviously different for the compared electrodes. The
211 values obtained for the SGDE were 22.7 % and 10.5 % lower than those for the SE at
212 the applied potentials of -1.2 V and -1.3 V, respectively. In addition to the resistances,
213 the values of capacitances Q_1 and Q_2 obtained from the SGDE were approximately
214 two to three times higher than that from the SE, respectively. It suggests that a larger
215 electrochemically active surface area could be provided by the SGDE compared to the
216 SE for ERCF [33]. Taking into account the structural changes from SE to SGDE, the
217 decrease in R_2 value and increase in capacitances may be related with an enhanced
218 CO_2 working concentration in the vicinity of the electrocatalytically active sites.

219 3.3 ERCF in MEC

220 As already mentioned, the MEC reactor was a two-chambered MFC operating in

electrolysis mode. The performance characteristics of this MFC are presented in Figure S7. The open circuit voltage (OCV) and the maximum power density were 0.638 V and 745 mW m^{-2}, respectively. These values are comparable to those obtained with similar configurations in other studies [25, 34].

In MEC mode, both electrodes are compared as it concerns ERCF according to the Faraday efficiency (FE_{HCOOH}) and production yield of formic acid. It can be seen that ERCF occurred with both electrodes when the applied cathode potential was negative than -1.0 V (Figure 4). In addition, the SGDE performed better than the SE for ERCF over the entire range of the applied cathode potentials. The maximum FE_{HCOOH} value of 40.09 ± 3.91 % and formic acid production yield of 0.064 ± 0.006 mol m^{-2} were both obtained with the SGDE at the applied cathode potential of -1.2 V. They were 36.1 % and 30.6 % higher than those obtained with the SE (FE_{HCOOH} value: 29.45 ± 2.21 %, production yield: 0.049 ± 0.005 mol m^{-2}). Comparing with the SE (i.e. a metal cathode), the SGDE could significantly promote ERCF in MEC, which is reported here for the first time.

4. Discussion

When the SE cathode is used for ERCF in aqueous electrolyte, CO_2 is provided by sparging in the catholyte bulk. In that case, the absorbed CO_2 (ad), as the main reactant of ERCF will be limited by the low solubility of CO_2 in water (ca. 0.033 M) (formation path of CO_2 (ad): CO_2 (g) → CO_2 (aq) → CO_2 (ad)). Moreover, the species CO_2(aq) reacts with OH^- to produce HCO_3^- and CO_3^{2-} ions, decreasing the CO_2 (ad) concentration [35]. The aforementioned limitation of CO_2 mass transfer (e.g. low CO_2

(ad) concentration) can be greatly broken by using the SGDE, where a direct formation path of CO_2 (ad) from the gaseous state (CO_2 (g) → CO_2 (ad)) is allowed (see Figure S8). So that an effective increase in the concentration of CO_2 (ad) at the electrochemically active sites can be achieved [35]. It was confirmed by the results of CV and EIS in this work where a higher ERCF current and lower charge transfer resistance were obtained by using the SGDE compared to the SE. The advantages of the SGDE are also supported by the results of the ERCF experiments in MEC, where the FE_{HCOOH} value and production yield of formic acid were enhanced by 36.1 % and 30.6 %, respectively when using the SGDE cathode to replace the SE cathode. In order to explore the performance of the SGDE without consideration of the bioanode activity, ERCF experiments in CEC were also carried out using a more negative potential region (from -1.2 V to -2.0 V) (Figure S9). The maximum FE_{HCOOH} value of 79.27 ± 1.52 % and current density of 17.57 ± 1.05 mA cm^{-2} were obtained from the SGDE, which were higher than those from the SE by 25.4 % and 61.5 %, respectively. The FE_{HCOOH} value of 79.27 ± 1.52 % is the highest reported in literature when using Sn electrodes under the same conditions [5, 18, 36-39]. It is clear that the CO_2 mass transfer limitation was indeed alleviated by using the SGDE. Other than the CO_2 mass transfer limitation, high energy consumption is also a significant barrier of ERCF in the current studies. In our experiments, by using the SGDE cathode for ERCF in MEC, the input voltage reached 0.66-0.82 V during electrolytic period of 2 h at the applied cathode potential of -1.0 V (Figure S10), approximately 67.2-73.6 % lower than the value by using a typical Sn GDE cathode in CEC at ambient pressure

(ca. 2.5 V [8]). Obviously, the energy consumption for ERCF is greatly reduced by the use of SGDE as well as MEC.

It has been explained that why the typical GDEs in the current studies in ERCF are incapable of good electron conduction and CO_2 diffusion. Then we developed the two-layer structure of the SGDE, anticipating an improvement in the current collection by using the brass mesh and in CO_2 diffusion by decreasing the thickness of the catalyst film. In order to confirm that, ERCF tests in CEC with a typical three-layer Sn GDE cathode were also carried out at the cathode potential of -1.8 V. The GDL of this Sn GDE was the same as that of the SGDE. The CL of this Sn GDE was prepared by spraying the as-prepared Sn catalyst ink onto the GDL, described in our previous work [27]. The FE_{HCOOH} value of 63.48 ± 3.31 % and current density of 10.56 ± 3.12 mA cm^{-2} obtained from the Sn GDE were 19.9 % and 39.9 % lower than that obtained from the SGDE, respectively. This indicates that the novel SGDE indeed alleviates the problems of electron conduction and CO_2 diffusion found in ERCF with the typical Sn GDE of three-layer structure. Other advantages of the SGDE such as low fabrication cost (ca. 30 \$ m^{-2}) and simple fabrication procedure are undoubtedly favorable for the future industrial application.

In this work, the high energy consumption and CO_2 mass transfer limitation for ERCF are greatly reduced owing to the MEC with SGDE cathode. In that system, industrial waste gases could act as CO_2 sources at SGDE cathode and the CO_2 released from the biodegradation process of the organic matters in real wastewaters at the bioanode could be recovered. Most importantly, by using a SGDE cathode in a MEC, ERCF can

work favorably while wastewaters can be effectively treated.

5. Conclusions

A two-layer rolled Sn-loaded gas diffusion electrode (SGDE) consisting of a gas diffusion layer and Sn-loaded brass mesh was developed to improve electrochemical reduction of CO_2 to formic acid (ERCF) in microbial electrolysis cell (MEC). Sn catalyst existed in the forms of SnO_2 and Sn, in the external and the internal of the Sn-loaded brass mesh, respectively. Compared to the Sn-loaded brass mesh (SE), the SGDE has advantages, including higher ERCF current and lower charge transfer resistance. A maximum Faraday efficiency of 40.09 ± 3.91 % % and a production yield of 0.064 ± 0.006 mol m^{-2} were achieved in MEC with the SGDE cathode, which were 36.1 % and 30.6 % higher than those obtained in MEC with the SE cathode. This enhanced performance can be attributed to the unique structure of the SGDE which alleviates the CO_2 mass transfer and electron conduction limitations. Other advantages of the SGDE, such as the low fabrication cost (ca. 30 \$ m^{-2}) and the simple fabrication procedure are also beneficial for its industrial application. Using the SGDE in a MEC, ERCF can be carried out favorably with low energy consumption while wastewaters can be effectively treated. In a following work, long-term experiments will be carried out to make ERCF in MEC with SGDE cathode more reliable for CO_2 conversion.

Acknowledgements

The authors gratefully acknowledge financial support by the Major National Science & Technology Projects of China on Water Pollution Control and Treatment (2012ZX07501002-001) and Research Project of Tianjin City for Application

Foundation and Advanced Technology (BE026071).

References

1. Y. Chen and M. W. Kanan, *J Am Chem Soc*, 2012, 134, 1986-1989.
2. J. H. Jeon, P. M. Mareeswaran, C. H. Choi and S. I. Woo, *RSC Advances*, 2014, 4, 3016.
3. Y. Koo, R. Malik, N. Alvarez, L. White, V. N. Shanov, M. Schulz, B. Collins, J. Sankar and Y. Yun, *RSC Advances*, 2014, 4, 16362.
4. Y. Kwon and J. Lee, *Electrocatalysis*, 2010, 1, 108-115.
5. C. Oloman and H. Li, *ChemSusChem*, 2008, 1, 385-391.
6. J. Qiao, P. Jiang, J. Liu and J. Zhang, *Electrochemistry Communications*, 2014, 38, 8-11.
7 Zhao, H.; Zhang, Y.; Zhao, B.; Chang, Y.; Li, Z., *Environ. Sci. Technol.* 2012, 46, 5198-5204.
8. D. T. Whipple, E. C. Finke and P. J. Kenis, *Electrochemical and Solid-State Letters*, 2010, 13, B109-B111.
9. Y. Jiang, M. Su, Y. Zhang, G. Zhan, Y. Tao and D. Li, *International Journal of Hydrogen Energy*, 2013.
10. B. E. Logan, *ChemSusChem*, 2012, 5, 988-994.
11. B. E. Logan, B. Hamelers, R. Rozendal, U. Schröder, J. Keller, S. Freguia, P. Aelterman, W. Verstraete and K. Rabaey, *Environmental science & technology*, 2006, 40, 5181-5192.
12. A. W. Jeremiasse, H. V. M. Hamelers, E. Croese and C. J. N. Buisman, *Biotechnology and Bioengineering*, 2012, 109, 657-664.
13. L. Lu, D. Xing, T. Xie, N. Ren and B. E. Logan, *Biosensors & Bioelectronics*, 2010, 25, 2690-2695.
14. S. Cheng, D. Xing, D. F. Call and B. E. Logan, *Environmental science & technology*, 2009, 43, 3953-3958.
15. H.-Z. Zhao, Y. Zhang, Y.-Y. Chang and Z.-S. Li, *Journal of Power Sources*, 2012, 217, 59-64.
16. B. Y. Chen, *Aerosol and Air Quality Research*, 2013, DOI: 10.4209/aaqr.2012.05.0122.
17. A. Li, H. Wang, J. Han and L. Liu, *Frontiers of Chemical Science and Engineering*, 2012, 6, 381-388.
18. R. L. Machunda, H. Ju and J. Lee, *Current Applied Physics*, 2011, 11, 986-988.
19. G. K. S. Prakash, F. A. Viva and G. A. Olah, *Journal of Power Sources*, 2013, 223, 68-73.
20. M. Mahmood, D. Masheder and C. Harty, *Journal of applied electrochemistry*, 1987, 17, 1159-1170.
21. J. Wu, P. P. Sharma, B. H. Harris and X.-D. Zhou, *Journal of Power Sources*, 2014, 258, 189-194.
22. R. A. Rozendal, H. V. Hamelers, K. Rabaey, J. Keller and C. J. Buisman, *Trends in biotechnology*, 2008, 26, 450-459.
23. W. Lv, R. Zhang, P. Gao, C. Gong and L. Lei, *Journal of Solid State Electrochemistry*, 2013, 17, 2789-2794.
24. H. Dong, H. Yu, X. Wang, Q. Zhou and J. Feng, *Water Res*, 2012, 46, 5777-5787.
25. X. Peng, H. Yu, X. Wang, N. Gao, L. Geng and L. Ai, *Journal of Power Sources*, 2012.
26. X. Wang, S. A. Cheng, Y. J. Feng, M. D. Merrill, T. Saito and B. E. Logan, *Environ. Sci. Technol.*, 2009, 43, 6870-6874.
27. Q. Wang, H. Dong and H. Yu, *RSC Adv.*, 2014, 104, 59970 - 59976.

28. S. Zhang, P. Kang and T. J. Meyer, *J Am Chem Soc*, 2014, 136, 1734-1737.
29. Y. Chen and M. W. Kanan, *Journal of the American Chemical Society*, 2012, 134, 1986-1989.
30. S. Kapusta and N. Hackerman, *Electrochimica Acta*, 1980, 25, 1625-1639.
31. Fu.Wang, F. Xie and R. Hu, *Anal Bioanal Chem, 2007,* 387, 933 – 939.
32. W. Lv, R. Zhang, P. Gao and L. Lei, *Journal of Power Sources*, 2014, 253, 276-281.
33. M. Mirzaeian and P. J. Hall, *Journal of Power Sources*, 2010, 195, 6817-6824.
34. X. Peng, H. Yu, X. Wang, Q. Zhou, S. Zhang, L. Geng, J. Sun and Z. Cai, *Bioresource technology*, 2012, 121, 450-453.
35. R. Chaplin and A. Wragg, *Journal of applied electrochemistry*, 2003, 33, 1107-1123.
36. J. Qiao, Y. Liu, F. Hong and J. Zhang, *Chem Soc Rev*, 2014, 43, 631-675.
37. A. S. Agarwal, Y. Zhai, D. Hill and N. Sridhar, *ChemSusChem*, 2011, 4, 1301-1310.
38. M. Alvarez-Guerra, S. Quintanilla and A. Irabien, *Chemical Engineering Journal*, 2012, 207–208, 278-284.
39. J. Wu, F. G. Risalvato, F. S. Ke, P. J. Pellechia and X. D. Zhou, *Journal of the Electrochemical Society*, 2012, 159, F353-F359.

Figure Captions

Figure 1 SEM images of the SGDE (a), catalyst particles (b), and crossover section of the Sn-loaded brass mesh (c).

Figure 2 CVs obtained with the SGDE and the SE in 0.5 M $KHCO_3$ in N_2 environment (a) and CO_2 environment (b) at a scan rate of 0.1 V s^{-1}. The inserted plots show the oxidation peaks between -0.8 V and -1.1 V obtained with the SE in N_2 environment.

Figure 3 Nyquist plots for the SGDE and the SE at an applied potential of -1.2 V and -1.3 V.

Figure 4 Dependence of Faraday efficiency and formic acid production yield on applied cathode potential in MEC mode.

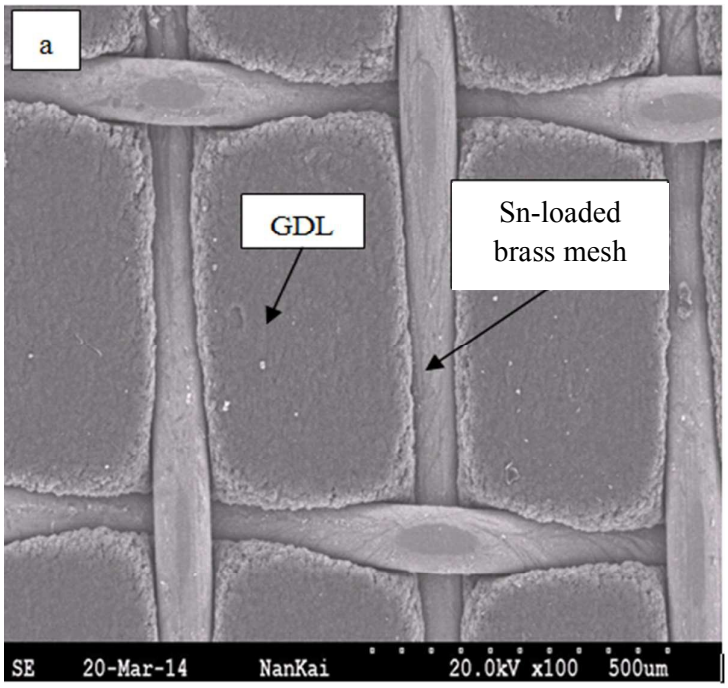

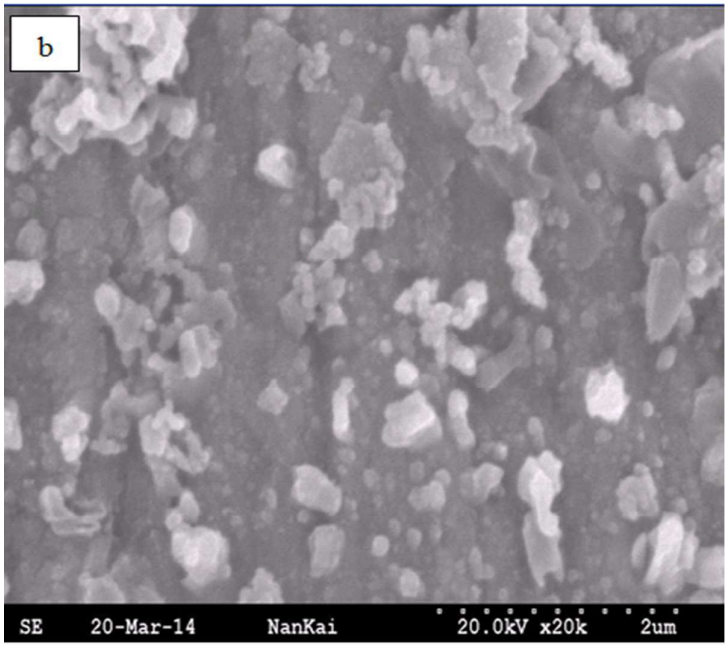

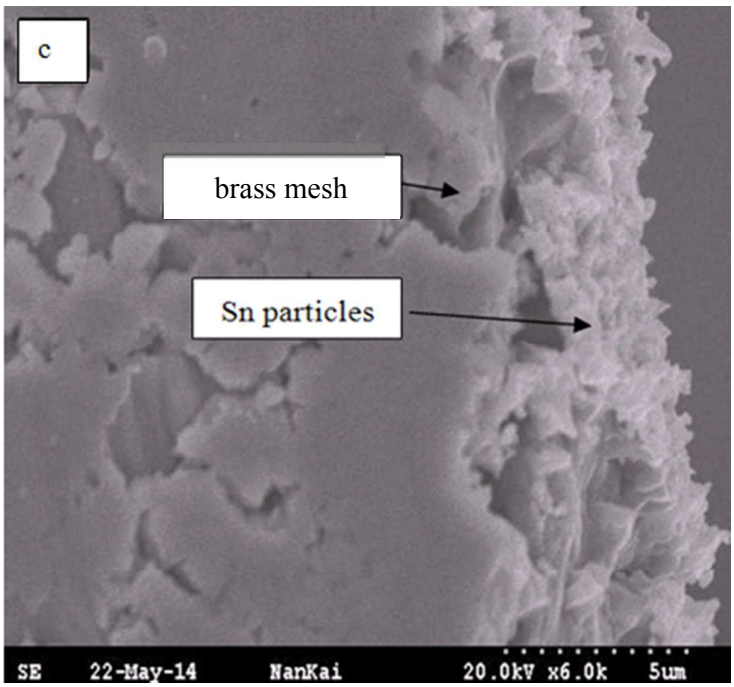

Figure 1

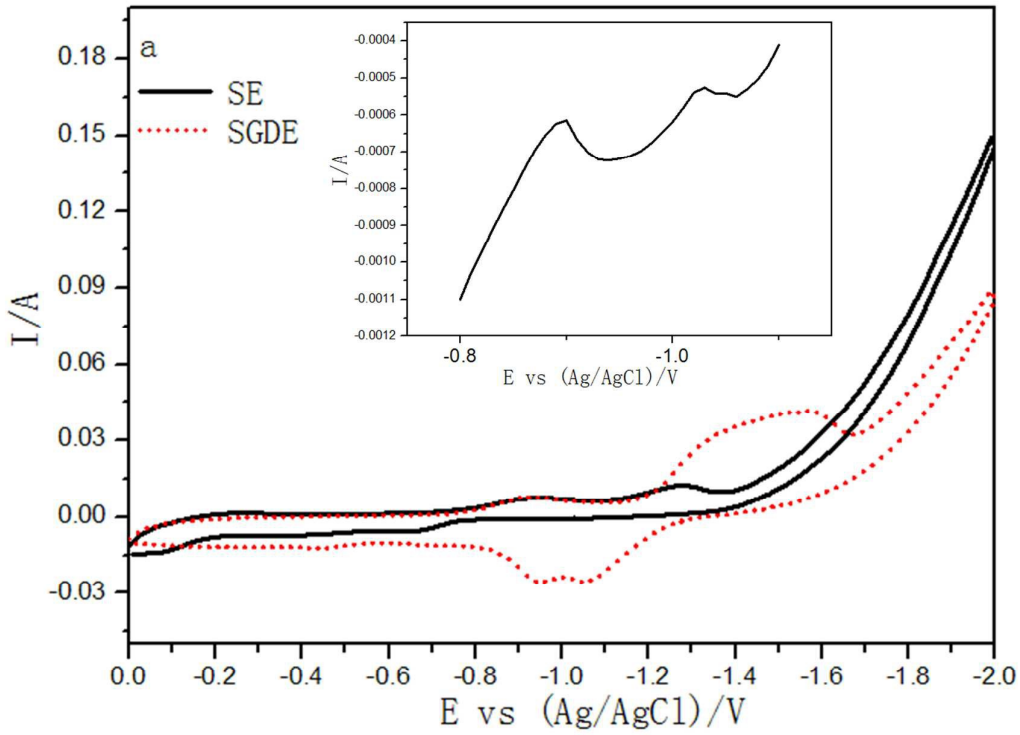

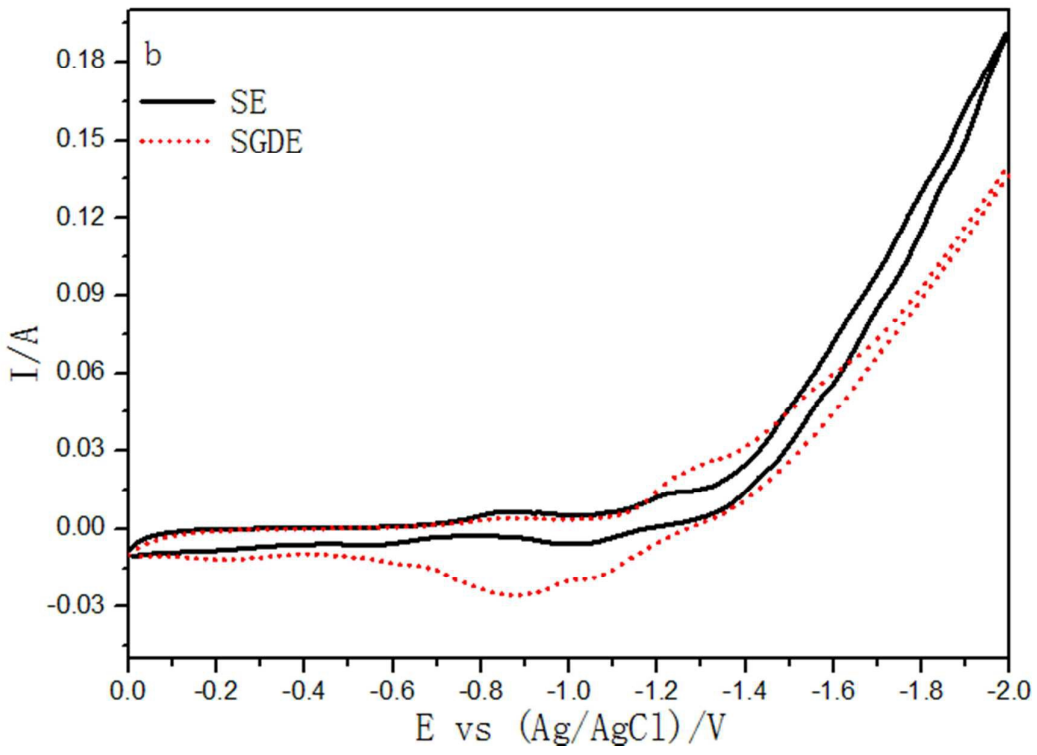

384

385 **Figure 2**

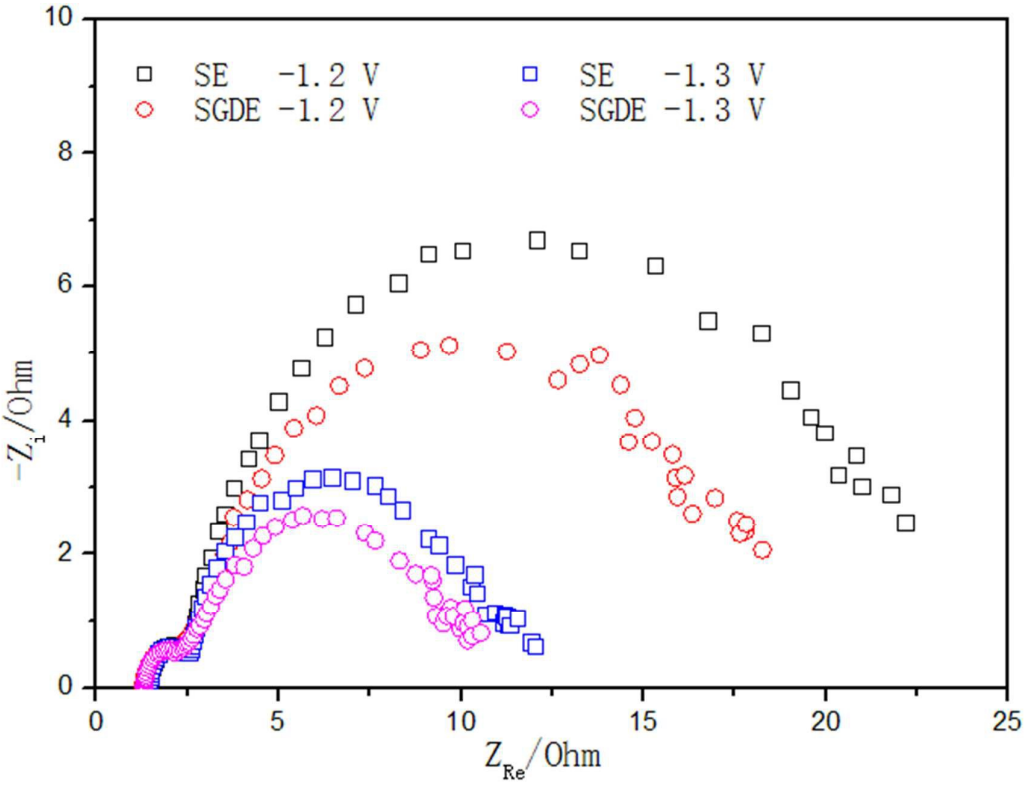

386

387 **Figure 3**

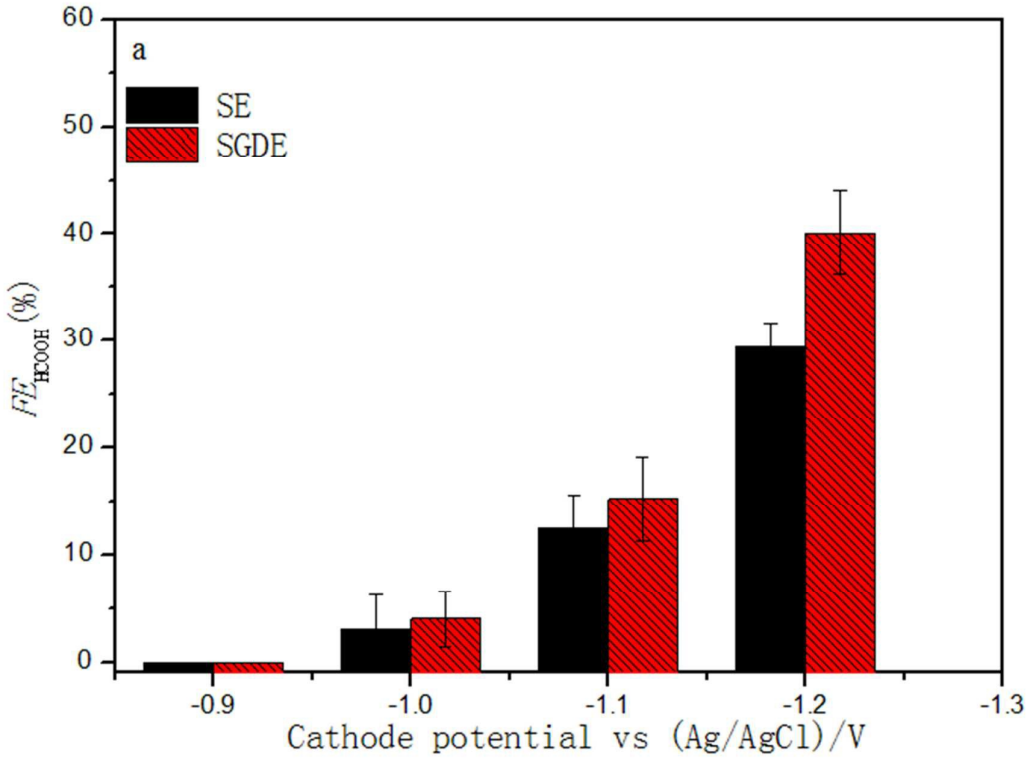

388

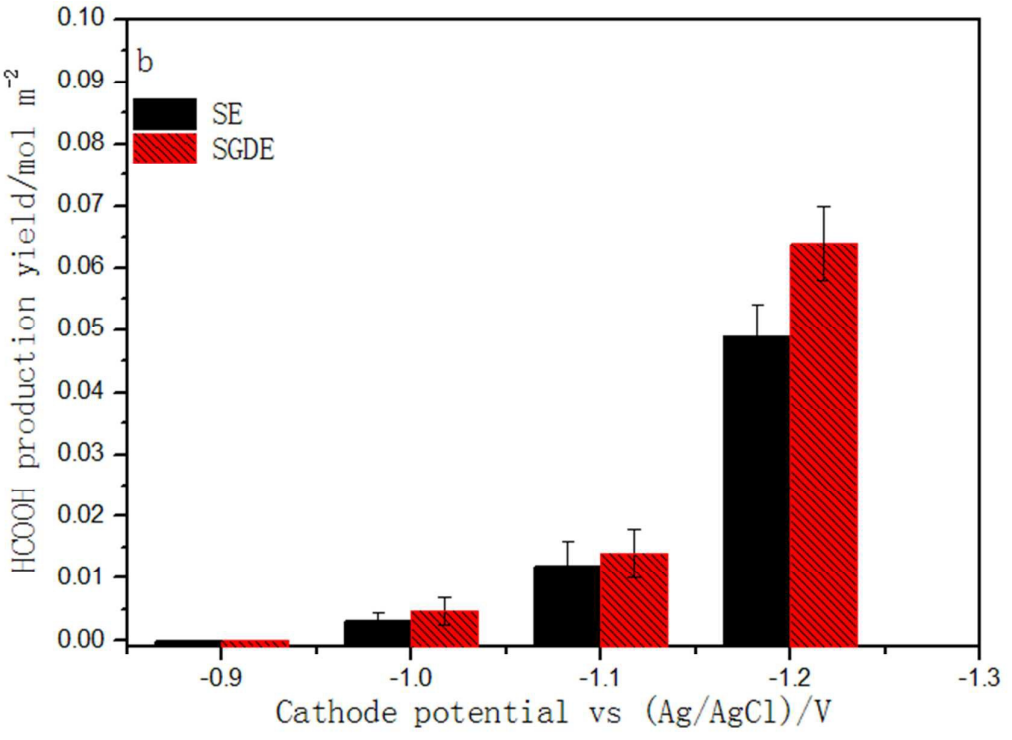

389

390 **Figure 4**